The impact of volcanic eruptions on ocean pH

Holly Olivarez

Senior, Fall 2018: Department of Earth & Planetary Sciences, University of New Mexico

SOARS® Summer 2018

Science Research Mentor: Nikki Lovenduski
Writing and Communication Mentor: B.J. Smith
Computing Mentor: Elizabeth Maroon
Coach: Syuan Wang
Peer Mentor: Jeremiah Piersante

ABSTRACT

Volcanic eruptions can have a major influence on the Earth system. Aerosols, gas molecules, and fine ash particles from large explosive eruptions can remain in the stratosphere for months to years, decreasing incoming solar radiation and causing Earth's surface to cool. Eruption records reflect temperature decreases significant enough to disrupt the water cycle and reduce atmospheric carbon dioxide concentrations. The impact of volcanic eruptions on ocean biogeochemistry has not been well studied, yet there is a pressing need to explore this topic because volcanic eruptions are analogous to radiation management geoengineering schemes and to the climate effects of a potential nuclear conflict. Understanding these effects may also help us understand the effects of past asteroid collisions with the Earth. Using output from the Community Earth System Model Large Ensemble (CESM-LE), which includes atmospheric and biogeochemistry components, we investigated the effects of three major volcanic eruptions in the past (Agung 1963, El Chichón 1982, Mount Pinatubo 1991) on the modeled ocean potential hydrogen (pH.) Ocean pH is a measure of ocean acidity that is closely tied to temperature, salinity, and carbon dioxide solubility in seawater. We show that sea surface temperatures decrease following a volcanic eruption (see figure below) and global ocean pH rises in the next two to three years. We further show this effect is amplified in the equatorial Pacific as a result of slower upwelling of corrosive water during an El Niño-like event, which supports current scientific discussion regarding El Niño-like responses following a volcanic eruption.

This work was performed under the auspices of the Significant Opportunities in Atmospheric Research and Science Program. SOARS is managed by the University Corporation for Atmospheric Research and is funded by the National Science Foundation, the National Center for Atmospheric Research, the National Oceanic and Atmospheric Administration, and the University of Colorado at Boulder.

1. Introduction

Volcanic eruptions can have a dramatic impact on the Earth system: sulfur aerosols from these eruptions interact with solar radiation and are then scattered into space, which contributes to cooling at the Earth's surface (Schneider et al., 2009). The 1991 Mount Pinatubo eruption, for example, injected approximately 20 megatons of sulfur dioxide into the atmosphere. A massive aerosol cloud circled the globe in three weeks and led to a two-year reversal of the late 20th century warming trend (Robock, 2000). Reflection of light by volcanic aerosols caused reduced radiative forcing by about 4.5 W m^{-2} following Mount Pinatubo's explosion (Hansen et al., 1992) compared to the mean supply of 237 W m^{-2}. Paleoclimate data and observations incorporated into climate simulation models have helped scientists understand short- and long-term effects of volcanic eruptions when addressing warming/cooling trends and global precipitation (Schneider et al., 2009). Model simulations have been used recently to study potential impacts of tropical volcanic eruptions on stimulating El Niño-like conditions in the tropical Pacific (Eddebbar et al., 2018). However, the literature includes no published studies of the impact of volcanic eruptions on ocean acidity. Ocean acidity, or potential hydrogen (pH), is related to the solubility of carbon dioxide, temperature, and salinity in seawater. Atmospheric injections from volcanic eruptions serve as analogs for proposed radiation management geoengineering schemes, as well as the climate effects of potential nuclear conflict (i.e., nuclear winter as described by Robock (2010)).

This paper examines the impact of volcanic eruptions on ocean pH. We do this computationally, using a global climate simulation, to investigate the effects of three major volcanic eruptions (Agung 1963, El Chichón 1982, and Mount Pinatubo 1991; see Table 1 for a description) on modeled ocean pH. Our research focuses on the coupled climate model Community Earth System Model Large Ensemble (CESM-LE), which includes atmospheric and biogeochemistry components, as described in Methods Section 2. In Section 3, we review the hypothesis for this experiment. We conclude with the results and a discussion in Section 4.

Volcanic Eruption	Date	Location	VEI	DVI
Agung, Indonesia	March 17, 1963	8°S 115°E	4	800
El Chichón, Mexico	April 4, 1982	17°N 93°W	5	800
Mount Pinatubo, Philippines	June 15, 1991	15°N 120°E	6	1000

Table 1: A list of the three volcanic eruptions included in CESM-LE simulations. Table includes the Volcanic Explosivity Index (VEI), a relative measure of explosiveness by Simkin and Siebert (1994); also, the Dust Veil Index (DVI), a numerical index that quantifies the impact of a volcanic eruption's release of dust and aerosols over the years following the event (Lamb, 1983).

2. Methods

a. Climate Models

Since 1983, the National Center for Atmospheric Research (NCAR) has offered multiple versions of a freely available global atmosphere model for use by the wider research community. The Community Earth System Model version 1 (CESM1), released in 2015, is a coupled climate model for simulating Earth's climate system. The model is composed of four separate models

synchronously simulating Earth's land, atmosphere, ocean, and sea ice, plus one central coupler component (UCAR n.d.).

The model consists of a system of differential equations that describe fluid motion, radiative transfer, and more. The planet is divided into a three-dimensional grid to solve the equations. Land, atmosphere, ocean and sea ice are traditionally at the same 0.25°, 1°, and 2° resolutions, on a 30-minute time step for 1° and 2° resolutions, 32 atmosphere layers, 60 ocean layers (0.1° or 1°), and 25 ground layers (Lamarque, 2017). Changes in external forcing can be applied (such as solar input, greenhouse gases, and volcanic eruptions, as will be discussed). The sub-gridscale processes (physical processes that occur at smaller scales that cannot be properly modeled, such as convection, land surface processes, albedo, hydrology, and cloud cover) are averaged over the larger scale, a technique known as parameterization. The setup provides for a virtual laboratory for experimentation (Holland, 2013).

b. The Large Ensemble Experiment

In discussing climate models in 2009, Schneider et al. reported the difficulty of separating internal variability from volcanic eruptions. This problem was resolved in 2015 when Kay et al. released the Community Earth System Model Large Ensemble (CESM-LE) to allow for recent-past and near-future climate change research in the presence of internal climate variability (processes such as ocean currents, for example), and for model error. CESM-LE simulates climate trajectories over 1920-2005 with slightly different air temperature initiations. Sometime after the initial condition memories are forgotten, each of the 36 ensemble members follows a different path in response to atmospheric changes.

Simulation trajectories cover 1,032 months (January 1, 1920, to December 31, 2005, with no leap years) and are referred to as the historical run. Sea surface temperatures and surface pH output were analyzed. Surface pH values are considered to encompass from zero to 10 meters in the ocean.

b-i. Atmospheric component

The atmosphere component used by CESM-LE is Community Atmosphere Model version 5 (CAM5), is integrated at a 1° X 1° horizontal resolution (Hurrell et al., 2013). CAM5 is able to simulate the cloud-aerosol indirect radiative effects (Neale et al., 2004).

In CESM-LE, as each of the ensemble members experiences the same external forcing (including the aerosol loading following volcanic eruptions), the ensemble mean captures the response to volcanic eruptions, which then reflects the divergence across the ensemble members as related to internal variability alone.

b-ii. Ocean and ocean biogeochemistry components

CAM5 is coupled to the CESM1 ocean component named the Parallel Ocean Program, version 2 (POP2; Smith et al., 2010). The model is defined at approximately 1° horizontal resolution and 60 vertical levels (Lovenduski et al., 2016), and includes full carbonate system dynamics,

allowing for computation of inorganic carbon chemistry, oceanic pCO_2, and air-sea CO_2 and O_2 fluxes (Moore et al., 2013), which reflect physical transport, solubility variations, net community production, and ocean-atmosphere exchange (Doney et al., 2008). Ocean carbon biogeochemistry is simulated using the ocean Biogeochemical Elemental Cycling (BEC) model, which is coupled to POP2.

Long et al. (2013) describe the computations of oceanic dissolved inorganic carbon (DIC), deep-ocean drift, biases related to freshwater inventories, biases in surface variables that affect ocean CO_2 update, climate-driven variability in carbon cycle dynamics, and sea-air exchange of CO_2. The model advects dissolved inorganic carbon, alkalinity, temperature, and salinity tracers and solves the full system of seawater carbonate chemistry equations at each model grid and time step. In this way, the model predicts ocean pH as a function of changing environmental conditions.

Skill assessments comparing field measurements and remote sensing data against BEC are reported by Doney et al., 2008. Analysis of regional and temporal variability in air-sea fluxes and ocean carbon uptake and storage are evaluated by Long et al., 2013. Further model validation, including comparison to observations for carbon cycle and surface productivity metrics, has been performed by Friedrichs et al., 2007, and Moore et al., 2004 and 2013.

c. Volcanic Eruptions in the Large Ensemble

The volcanic radiative forcing in CESM-LE uses the forcing dataset of Ammann et al. (2003), which includes an aerosol optical depth at 0.5 micron (500 nm) based on the quantity of sulfate injected into the atmosphere by each eruption, but also considers the seasonally changing transport of atmospheric aerosols.

As mentioned previously, we use 36 ensemble members to examine the ocean acidity's response to the external forcing of three large volcanic eruptions: Agung 1963, El Chichón 1982, and Mount Pinatubo 1991. Similar to the summation of CESM-LE made by Long et al. (2016), CESM-LE's format aids in seeing forced signals overlaid over natural variability. Figure 1 represents an example of this. Global mean sea surface temperatures and pH values from 1950-2005 reflect each of the three volcanic eruptions written into the model, allowing for analysis of not only the eruptions, but also the natural variability.

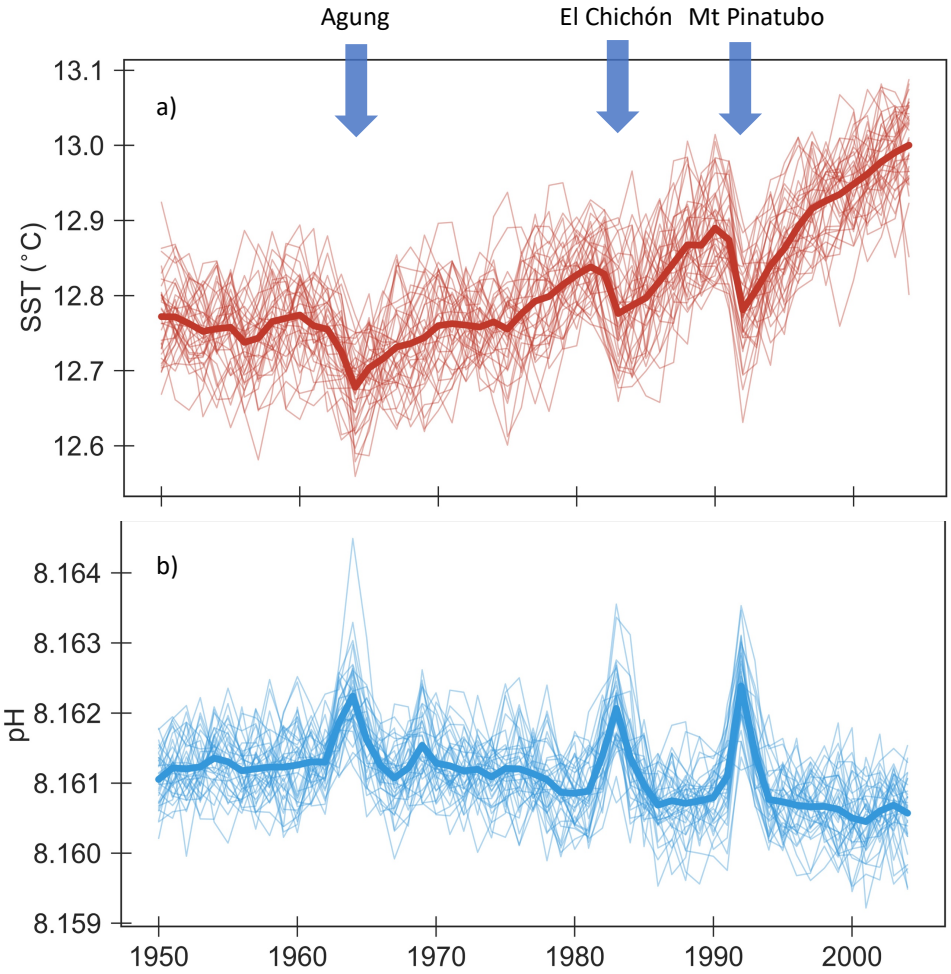

Figure 1. Community Earth System Model Large Ensemble (CESM-LE) 1950-2005: a) global mean sea surface temperatures (SST), b) global mean surface pH values using natural (pre-industrial) atmospheric carbon dioxide concentration (280 parts per million). Each thin line represents annual means of one of 36 ensemble members; bold line represents mean of all ensemble members. All three volcanic eruptions are seen as sea surface temperatures drop and pH values rise in 1963 (Agung), 1982 (El Chichón), and 1991 (Mount Pinatubo).

Anthropogenic carbon dioxide concentrations increased in the time frame of the three volcanic eruptions from 1950-2005, resulting in a long-term decrease in ocean pH (see Figure 2). In order to quantify the response of ocean pH due to volcanic eruptions, we use output that includes only pre-industrial atmospheric carbon dioxide concentration values of 280 parts per million (herein referred to as natural pH).

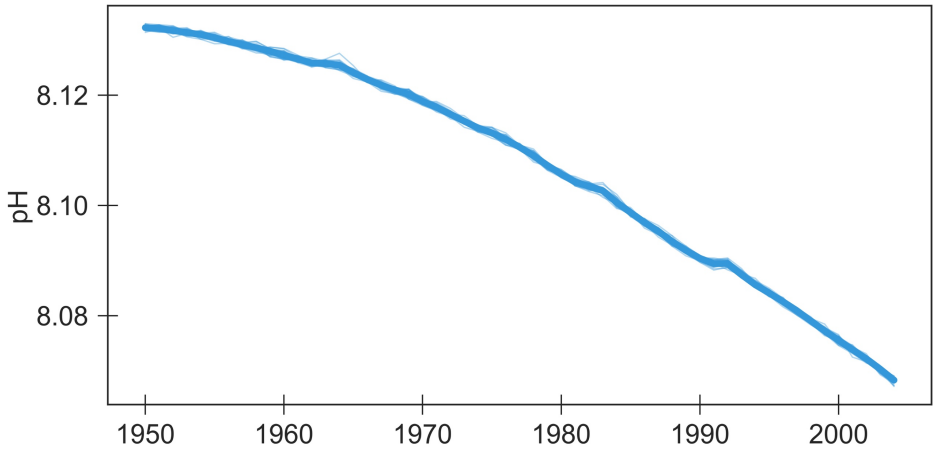

Figure 2. CESM-LE global mean pH values from 1950-2005 using contemporary (anthropogenic plus natural) atmospheric carbon dioxide (CO_2) values. The effect of ocean acidification due to global climate change can be seen much more strongly than the signals from the three volcanic eruptions.

3. Hypothesis

Potential hydrogen, or pH, is approximately the negative of the base 10 logarithm of the molar concentration, measured in units of moles per liter, of hydrogen ions. A difference of one pH unit is equivalent to a tenfold difference in the hydrogen ion concentration.

Ocean pH is closely tied to carbon dioxide solubility in seawater. In addition to the carbon dioxide concentration, pH (= $-\log_{10}[H+]$) is also related to the temperature and salinity of seawater through the equilibrium constants of three chemical reactions:

CO_2 ↓

$CO_2 + H_2O$	⟷	H_2CO_3	Carbonic acid
H_2CO_3	⟷	$HCO_3^- + H^+$	Bicarbonate
HCO_3^-	⟷	$CO_3^{2-} + H^+$	Carbonate

Figure 3 shows the resulting sensitivity of pH to temperature.

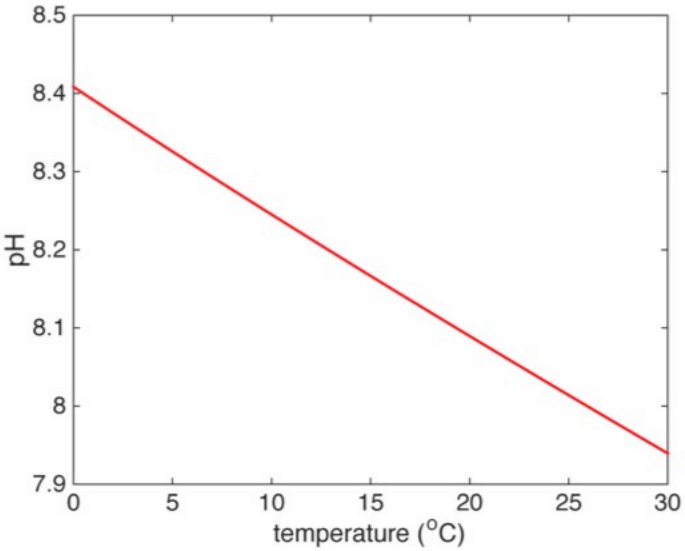

Figure 3. Temperatures from zero to 30 degrees Celsius are shown on the x-axis. The y-axis shows a range of ocean pH values from 7.9 to 8.5. As temperature decreases along the x-axis, pH values increase along the y-axis.

4. Results and Discussion

Massive, explosive volcanic eruptions affect the global ocean in the following two to three years. A quick change in the atmosphere and temperatures following a volcanic eruption results in a quick change in ocean pH. Such a relatively quick change in ocean chemistry (explained in Section 3) does not give marine life time to adapt, which can have short- and long-term effects on many species.

Figure 4. Twelve-month mean anomalies of pH a) one year, b) two years, and c) three years after the eruptions. Anomalies are calculated from one year prior to each eruption. Red colors indicate pH values have decreased; blue colors indicate pH values have increased.

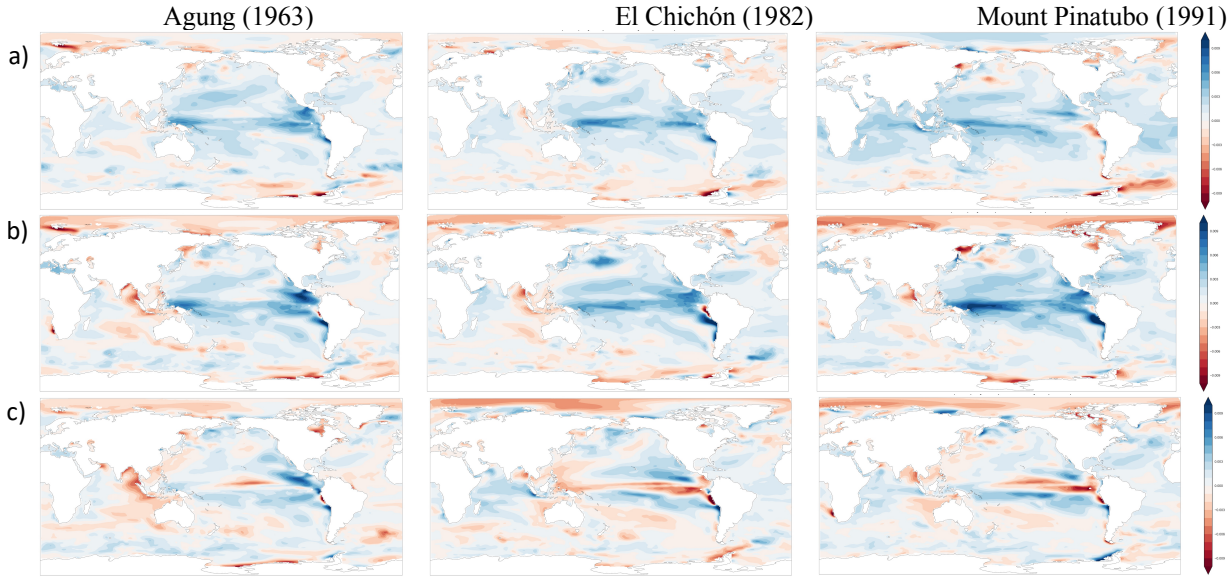

In examining the annual anomalies and seasonal responses (not shown), we found consistent responses amongst all three eruptions. Overall, we found an anomalous increase in global ocean surface pH that persists for two to three years following each eruption, though we observe large spatial variability in the response. Specifically, the first year following a volcanic eruption reflects a more basic ocean overall, with several regions having an opposite response of more acidic waters (see Figure 3). The second year following all eruptions, responses are amplified. The equatorial Pacific region seems to respond significantly in comparison with all other regions, as well as an equally contrasting response in the northern-most and southern-most latitudes. In the third year following an eruption, the pH values in the global ocean begin to recover. This study does not include analyses of the mid- to high-latitudes.

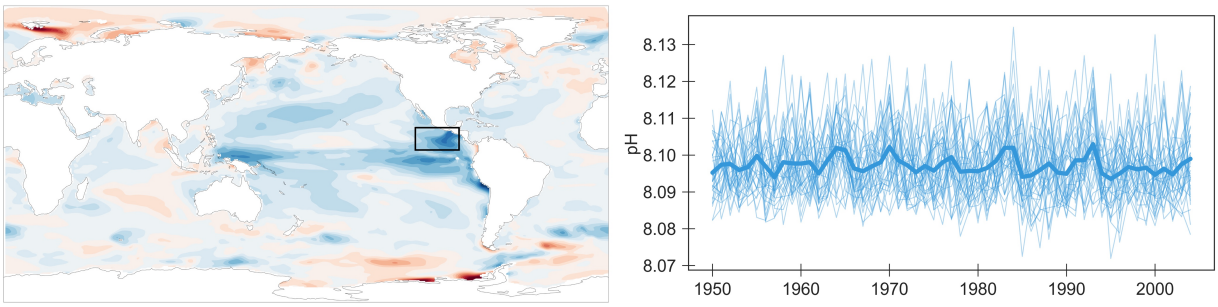

Figure 5. Left: Twelve-month mean anomalies of pH one year following the Agung (1963) eruption. Anomalies are calculated from one year prior to the eruption. Red colors indicate pH values have decreased; blue colors indicate pH values have increased. Black outline on figure reflects the region containing values depicted in figure on right. Right: Mean surface pH values using natural atmospheric carbon dioxide concentration (280 parts per million). Each thin line represents annual means of one of 36 ensemble members; bold line represents mean of all ensemble members. The peaks following each eruption (1963 Agung, 1982 El Chichón, 1991 Mount Pinatubo) reflect a 2-3-year response of rise in pH value.

In analyzing a region of the eastern Equatorial Pacific that appears to become much more basic than other areas of the world, there is significant climate variability amongst all 36 ensemble members (see Figure 5). We did, however, again find each ensemble member responds intensely following each eruption in this region. We also note the response following each eruption is maintained for a period of time (approximately 2 – 3 years) following each eruption.

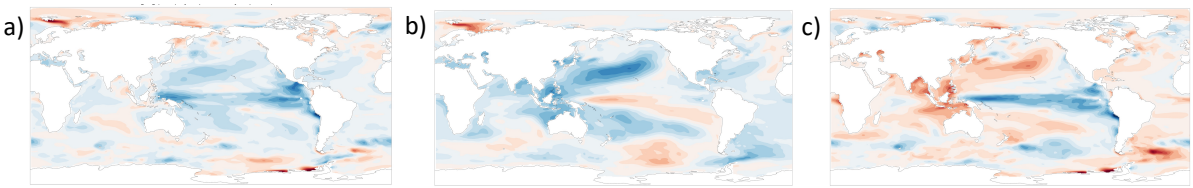

Figure 6. a) Global map of annual mean anomalies in pH one year after the Agung eruption compared to the year prior to the eruption, b) change in pH in response to change in sea surface temperatures, and c) change in pH in response to change in ocean circulation.

As shown in Figure 5, the anomalous increase in pH is primarily driven by decreasing ocean temperature in the subtropics and extra-tropics (Figure 5b). In the eastern Equatorial Pacific, however, the eruptions generate El Niño-like conditions and suppress the upwelling of corrosive water, leading to anomalously high pH (Figure 5c).

Our results verify recent (and under review) published papers that suggest that volcanic eruptions prompt El Niño-like events. Specific to tropical eruptions, Eddebbar et al. (submitted for review to *Journal of Climate*) refers to "volcanically forced El Niño behavior" and explains that the initiation of climatological upwelling of warm subsurface anomalies in the east that is responsible for the El Niño-like surface warming in the eastern and central tropical Pacific. Stevenson et al. (2016)'s detailed examination of the influences of volcanic eruptions using the CESM Last Millennium Ensemble verifies the cooling following an eruption persists for 2 – 3 years even in the tropics.

Our studies have further implications for climate geoengineering schemes, past asteroid impacts with the Earth, and the climate effects of potential nuclear conflict. They show that pH rises after externally forced events on the Earth system. Geoengineering by blocking the sun does not address current atmospheric carbon dioxide concentration levels or ocean acidification. Eddebbar et al. (submitted for review to *Journal of Climate*) suggests the reduction of ocean carbon uptake is a response to volcanic eruptions. As another potential consequence, the potential of the hydrological cycle being interrupted has been studied extensively by Trenberth and Stepaniak (2004), Trenberth and Dai (2007), Bala et al. (2008), and Robock (2008). In considering past asteroid impacts with the Earth, Robock (2010) proposes the dust cloud of of aerosols in Earth's atmosphere caused by an asteroid blocked out the Sun and is responsible for killing over 70% of the planet's species (the Cretaceous-Tertiary (K-T) extinction). In addition, Sarmiento (1993) suggests learning more about the effects of cooling can provide crucial insights that we may find are associated with global climate change. In other words, looking at the situation of global climate change from a different perspective may help our understanding of how to find solutions to current ocean acidification due to increasing carbon dioxide concentrations.

Acknowledgements

This work was performed under the auspices of the Significant Opportunities in Atmospheric Research and Science Program. SOARS is managed by the University Corporation for Atmospheric Research and funded by the National Science Foundation, the National Center for Atmospheric Research, the National Oceanic and Atmospheric Administration and the University of Colorado at Boulder.

We would like to thank Elizabeth Maroon for her computational assistance. Additional thanks to Kristen Krumhardt, Adi Johnson, and Jamin Rader.

Thank you to the Open Philanthropy Project.

The CESM project is supported by the National Science Foundation and the Office of Science (BER) of the U.S. Department of Energy. We would like to acknowledge high-performance computing support from Cheyenne (doi:10.5065/D6RX99HX) provided by NCAR's Computational and Information Systems Laboratory, sponsored by the National Science Foundation.

Computational and Information Systems Laboratory. 2017. Cheyenne: HPE/SGI ICE XA System (Climate Simulation Laboratory). Boulder, CO: National Center for Atmospheric Research. doi:10.5065/D6RX99HX.

References

Ammann, C., Meehl, G., and Washington, W. (2003). A monthly and latitudinally varying volcanic forcing dataset in simulations of 20th century climate. *Geophysical Research Letters*, 30, 12, 1-4, doi: 10.1029/2003GL016875

Bala, G., Duffy, P.B., and Taylor, K.E. (2008). Impact of geoengineering schemes on the global hydrological cycle. *Proceedings of the National Academy of Sciences of the United States of America,* 105, 22, 7664-7669, doi: 10.1073/pnas.0711648105

Eddebbar, Y., Rodgers, K., Long, M., Subramanian, A., Xie, S., and Keeling, R. (2018). El Niño-like physical and biogeochemical response to tropical eruptions, submitted for review to *Journal of Climate*.

Friedrichs, M.A.M., Dusenberry, J.A., Anderson, L.A., Armstrong, R.A., Chai, F., Christian, J.R., et al. (2007). Assessment of skill and portability in regional marine biogeochemical models: Role of multiple planktonic groups. *Journal of Geophysical Research,* 112, C8.

Gent, P.R., Danabasoglu, G., Donner, L.J., Holland, M.M., Hunke, E.C., Jayne, S.R., et al. (2011). The Community Climate System Model Version 4. *Journal of Climate*, 24, 19, 4973-4991, doi: 10.1175/2011JCLI4083.1

Gruber, N., and Doney, S. (2006). Ocean Biogeochemistry and Ecology (Second Edition). *Encyclopedia of Ocean Sciences*, 6, 89-104, doi: 10.1016/B978-012374473-9.00741-4

Hansen, J., Lacis, A., Ruedy, R., and Sato, M. (1992). Potential climate impact of Mount Pinatubo eruption. *Geophysical Research Letters*, 19, 215-218.

Holland, M. (2013). Introduction to the Community Earth System Model. Viewed 14 June 2018, http://www.cesm.ucar.edu/events/tutorials/2013/day1-lecture1-holland.pdf

Hurrell, J., Holland, M., and Gent, P.R. (2013). The Community Earth System Model: A framework for collaborative research. *American Meteorological Society*, September 2013, 1339-1360, doi: https://doi.org/10.1175/BAMS-D-12-00121.1

Kay, J.E., Deser, C., Phillips, A., Mai, A., Hannay, C., Strand, G., et al. (2015). The Community Earth System Model (CESM) Large Ensemble Project: A community resource for studying climate change in the presence of internal climate variability. *Bulletin of the American Meteorological Society*, 96, 1333-1349, doi: 10.1175/bams-d-13-00255.1

Lamarque, J.F. (2017). Introduction to the Community Earth System Model. Viewed 14 June 2018, http://www.cesm.ucar.edu/events/tutorials/2017/lecture1-lamarque.pdf

Lamb, H.H. (1983). Update of the chronology of assessments of the volcanic dust veil index. *Climate Monitor,* 12 (3), 79-90.

Lawrence, D. M., Oleson, K.W., Flanner, M.G., Fletcher, C.G., Lawrence, P.J., Levis, S., et al. (2012). The CCSM4 land simulation, 1850–2005: Assessment of surface climate and new capabilities. *Journal of Climate*, 25, 2240–2260, doi:10.1175 /JCLI-D-11-00103.1

Long, M.C., Lindsay, K., Peacock, S., Moore, J.K., Doney, S.C. (2013). Twentieth-century oceanic carbon uptake and storage in CESM1(BGC). *Journal of Climate*, 26, 18, 6775-6800, doi: 10.1175/JCLI-D-12-00184.1

Lovenduski, N.S., McKinley, G.A., Fay, A.R., Lindsay, K., and Long, M.C. (2016). Partitioning uncertainty in ocean carbon uptake projections: Internal variability, emission scenario, and model structure. *Global Biogeochemical Cycles*, 30, 9, 1276-1287, doi: 10.1002/2016GB005426

Moore, J.K., Doney, S.C., and Lindsay, K. (2004). Upper ocean ecosystem dynamics and iron cycling in a global three-dimensional model. *Global Biogeochemical Cycles,* 18, GB4028, doi: 10.1029/2004GB002220

Moore, J.K., Lindsay, K., Doney, S.C., Long, M.C., and Misumi, K. (2013). Marine ecosystem dynamics and biogeochemical cycling in the Community Earth System Model [CESM1(BGC)]: Comparison of the 1990s with the 2090s under the RCP4.5 and RCP8.5 scenarios. *Journal of Climate*, 26, 23, 9291-9312, doi: 10.1175/JCLI-D-12-00566.1

Neale, R.B., Chen, C.C., Gettelman, A., Lauritzen, P.H., Park, S., Williamson, D.L., et al. (2004). Description of the NCAR Community Atmosphere Model (CAM 5.0). *NCAR Technical Note-464+Str*, 1-274.

Robock, A. (2000). Volcanic eruptions and climate. *Reviews of Geophysics*, 38, 2, 191-219, doi: 10.1029/1998rg000054

Robock, A. (2008). 20 Reasons why geoengineering may be a bad idea. *Bulletin of the Atomic Scientists,* 64, 2, 14-18, 59, doi: 10.2968/064002006

Robock, A. (2010). Nuclear winter, *WIREs Climate Change*, 1, 418-427, doi.org/10.1002/wcc.45

Schneider, D.P., Ammann, C.M., Otto-Bliesner, B.L., Kaufman, D.S. (2009). Climate response to large, high-latitude and low-latitude volcanic eruptions in the Community Climate System Model. *Journal of Geophysical Research*, *114,* D15101, doi: 10.1029/2008jd011222

Simkin, T., and Siebert, L. (1994). Volcanoes of the world. *Geoscience, Tucson, Ariz.* 349 pp.

Smith, R., Jones, P., Briegleb, B., Bryan, F., Danabasoglu, G., Dennis, J., et al. (2010). The Parallel Ocean Program (POP) reference manual: Ocean component of the Community Climate

System Model (CCSM) and Community Earth System Model (CESM). Viewed 14 June 2018, http://cesm.ucar.edu.

Taylor, K.E., Stouffer, R.J., Meehl, G.A. (2012). An overview of CMIP5 and the experiment design. *Bulletin of the American Meteorological Society,* 93, 4, 485–498, doi: 10.1175/BAMS-D-11-00094.1

Trenberth, K.E., and Stepaniak, D.P. (2004). The flow of energy through the Earth's climate system. *Royal Meteorological Society,* 130, 603, 2677-2701, doi: 10.1256/qj.04.83

Trenberth, K.E., and Dai, A. (2007). Effects of Mount Pinatubo volcanic eruption on the hydrological cycle as an analog of geoengineering. *Geophysical Research Letters,* 34, L15702, doi: 10.1029/2007GL030524

UCAR n.d., *CEMS Models.* Viewed 12 June 2018, http://www.cesm.ucar.edu/models/ccsm4.0.